Available online at www.sciencedirect.com
ScienceDirect
Journal of Hazardous Materials 147 (2007) 265–274
Journal of Hazardous Materials
www.elsevier.com/locate/jhazmat

Selecting metal oxide nanomaterials for arsenic removal in fixed bed columns: From nanopowders to aggregated nanoparticle media

Kiril Hristovski [a,*], Andrew Baumgardner [b,1], Paul Westerhoff [b,2]

[a] *Environmental Technology Laboratory, Arizona State University—Polytechnic Campus, 7001 East Williamsfield Road Building 50, Mesa, AZ 85212, United States*
[b] *Department of Civil and Environmental Engineering, Arizona State University, Box 5306, Tempe, AZ 85287-5306, United States*

Received 17 August 2006; received in revised form 20 November 2006; accepted 1 January 2007
Available online 9 January 2007

Abstract

This paper investigates the feasibility of arsenate removal by aggregated metal oxide nanoparticle media in packed bed columns. Batch experiments conducted with 16 commercial nanopowders in four water matrices were used to select a metal oxide nanoparticle that both amply removes arsenate and can be aggregated using an inert binder. TiO_2, Fe_2O_3, ZrO_2 and NiO nanopowders, which exhibited the highest arsenate removal in all water matrices, were characterized with fitted Freundlich adsorption isotherm ($q = KC_e^{1/n}$) parameters. In 10 mM $NaHCO_3$ buffered nanopure water and at both pH ≈ 6.7 and 8.4, K ranged from 1.3 to 12.09 (mg As/g(media)) (L/mg As)$^{1/n}$, and $1/n$ ranged from 0.21 to 0.52. Under these conditions, the fitted Freundlich isotherm parameters for TiO_2 nanoparticles aggregated with inorganic and organic binders (K of 4.75–28.45 (mg As/g(media)) (L/mg As)$^{1/n}$ and $1/n$ of 0.37–0.97) suggested favorable arsenate adsorption. To demonstrate that aggregated nanoparticle media would allow rapid mass transport of arsenate in a fixed bed adsorber setting, short bed adsorber (SBA) tests were conducted on TiO_2 nanoparticle aggregates at empty bed contact times (EBCT) of 0.1–0.5 min and $Re \times Sc = 1000$ and 2000. These SBA tests suggested that the binder has a negligible role in adsorbing arsenic and that mass transport is controlled by rapid intraparticle diffusion rather than external film diffusion.

Keywords: Nanoparticle; Metal oxide; Arsenic; Water; Fixed bed column

1. Introduction

Since the discovery of buckyballs by Curl, Kroto, and Smalley in 1985, the new field of nanotechnology has rapidly emerged [1]. Nanotechnology, which is defined as "understanding and control of matter at dimensions of roughly 1–100 nm, where unique phenomena enable novel applications," is making a significant impact on our everyday lives [2]. Although nanotechnology has been used in fields such as medicine, biotechnology and electronics, its beneficial application to drinking water treatment has begun only recently [3–8].

Because of their size, nanomaterials can exhibit an array of novel properties that can be used to develop new technologies and improve existing ones. Characteristics such as large surface area, potential for self assembly, high specificity, high reactivity, and catalytic potential make nanoparticles excellent candidates for water treatment applications. In particular, efficient and less costly fixed bed absorbers incorporating nanomaterials as adsorbent material could remove contaminants from drinking water during municipal treatment or in point of use applications.

The performance of adsorbent media in a fixed bed column depends mainly on two factors: the adsorption capacity of the media and its mass transport kinetics. Since both factors can be limiting, nanomaterial fixed bed adsorption media could be designed to maximize mass transport kinetics by providing contaminants with rapid access to high surface area and by promoting internal mass transport. Since pore and surface diffusion generally control the internal mass transport, it is expected that usage of materials and shapes which facilitate these types of internal transport, to beneficially affect the mass transport kinetics.

* Corresponding author. Tel.: +1 480 727 1132; fax: +1 480 727 1684.
E-mail addresses: Kiril.Hristovski@asu.edu (K. Hristovski), BaumgardnerAC@bv.com (A. Baumgardner), p.westerhoff@asu.edu (P. Westerhoff).
[1] Tel.: +1 480 965 2885; fax: +1 480 965 0557.
[2] Tel.: +1 480 965 2885; fax: +1 480 965 0557.

0304-3894/$ – see front matter © 2007 Elsevier B.V. All rights reserved.
doi:10.1016/j.jhazmat.2007.01.017

External mass transport depends on particle size of the media, which can be controlled during the fabrication process. One way to engineer nanomaterial-based adsorbent media is to aggregate nanoparticles with inert binders. These cannot adversely affect the surface area, surface charge or composition of the metal oxide medium, however, because adsorption capacity depends on these factors. Therefore, this study evaluates the feasibility of using aggregated metal oxide nanoparticles as adsorbent media for arsenate removal in a fixed bed column setting.

Specific objectives are as follows: first, to select a metal oxide nanomaterial capable of ample arsenic removal; second, to demonstrate that introduction of a binder to aggregate the selected metal oxide nanoparticles does not adversely affect the adsorption capacity of the aggregate; and third, to evaluate the effect of binder type on the mass transport of arsenate into the aggregated media.

Arsenic was selected as a target contaminant because of its potential health and regulatory concerns as well as its ability to adsorb onto metal oxide surfaces by forming inner-sphere bidentate ligands. While most heavy metals occur as cations (Pb^{2+}, Cu^{2+}, Ni^{2+}, Cd^{2+}, Zn^{2+}, etc.) in water, arsenic is an oxy-anion-forming element (like Se, Sb, Mo, Cr, etc.) that is particularly unique in its sensitivity to mobilization at the pH values typically found in natural waters [9–11]. Although arsenic can exist in four different oxidation states (−3, 0, +3, and +5), As(V) is the prevalent form in oxygen-rich environments [11,12]. Under natural pH conditions, $H_2AsO_4^-$ and $HAsO_4^{2-}$ are the dominant As anions in water. As pH increases, so does the fraction of divalent and trivalent arsenate anions. Thus, treatment by adsorption is important because arsenic cannot be reduced to innocuous by-products like other oxy-anions, such as ClO_4^- or NO_3^-, can.

Arsenic is classified as a Class A human carcinogen by the International Agency for Research on Cancer (IARC) and is an emerging contaminant in water in many regions of the world [13–16]. Arsenic occurs naturally in soils and water, but it also enters the environment due to anthropogenic sources [11]. Many community water systems and private wells in North America and around the world have arsenic concentrations exceeding 10 μg/L, the maximum contaminant level (MCL) promulgated by the US EPA, European Union (EU) and World Health Organization (WHO) [17–21]. Regulatory pressure to reduce arsenic levels has spurred the development of technologies that economically remove arsenic from drinking water at during municipal treatment or in single dwelling, point of use applications.

2. Experimental approach

2.1. Characterization of the commercial nanopowders

Sixteen commercially available metal oxide nanopowders were obtained from Sigma–Aldrich (Table 1). These were selected as a base materials for comparison because their reported surface areas and sizes (see Table 1) implied that they are composed of discrete nanoparticles that are the same as or similar to those used in fabrication of nanoparticle aggregates. Before any adsorption experiments were conducted, the characteristics and behavior of the nanoparticles within aqueous environments was studied to develop procedures for their removal from water matrices.

Stock suspensions with concentrations of 1 g/L were prepared by suspending the nanopowders in nano-pure water with conductivity < 1.1 μS/cm and sonicating for 15 min in an ultrasonic bath at 90 W/L to allow disaggregation of the particles and homogenization of the suspension.

Nanopowder removal was evaluated by separating the nanopowder from the suspension via centrifugation (minimum 30 min at forces > 1300 G) and filtration with 0.2 and 2.5 μm pore size filters. The concentrations of the nanopowder supernatant and the filtrate were evaluated: (1) by light scattering at 250 nm and another wavelength determined by analysis of the metal oxide nanoparticle spectrum (Jenway UV/vis 6405, Felsted, UK); and/or (2) by digestion of the nanoparticles with HNO_3/H_2O_2 and Electro Thermal Atomic Adsorption

Table 1
Evaluated commercially available nanopowder metal oxides

Number	Nanopowder composition	Manufacturer reported surface area (m^2/g)	Manufacturer reported particle diameter (nm)	Estimated pH_{IEP} by phase analysis light scattering
1	Al_2O_3–I	350–720	2–4	8.8
2	Al_2O_3–II	35–43	40–47	6.3
3	Fe_2O_3	50–245	5–25	6.9
4	La_2O_3	N/A	<60	8.1
5	MgO	130	12.8	10.1
6	$MnTiO_3$	N/A	<60	4.2
7	NiO	50–80	10–20	10.7
8	SnO_2	47.2	18.3	3.7
9	TiO_2	190–290	15	5.9
10	WO_3	15–30	30–50	2.5
11	Y_2O_3	40–45	25–30	8.1
12	ZnO	15–25	50–70	9.1
13	$ZnFe_2O_4$	N/A	NA	8.2
14	ZrO_2	35–45	20–30	6.1
15	$ZnTiO_3$	40–45	<80	3.6
16	Fe_3O_4	>60	20–30	3.2

Table 2
pH, phosphorous concentrations, silica concentrations, and conductivities of the water matrices used in the screening experiments

Water	pH	Total P (μg/L)	Silica (mg/L)	Conductivity (μS/cm)
10 mM $NaHCO_3$ buffered nanopure water	8.4 ± 0.2	0	0	~900
Tap water (East Mesa, AZ)	8.1	NA	NA	~330
Groundwater (Well 4E, Scottsdale, AZ)	8.0 ± 0.2	<0.1	~25	~720
Surface water (CAP, AZ)	7.8	<0.1	~9	~950

Spectrophotometer (ET-AAS) analysis with a Varian Zeeman Spectra 400 Plus [22].

Table 1 presents the isoelectric points (IEP) of the nanopowders, which were evaluated by Phase Analysis Light Scattering (PALS) using a Brookhaven ZetaPALS instrument (Brookhaven Instrument Corporation, Holtsvile, NY). IEP measurements were conducted in 10 mM KNO_3 electrolyte solution; scanning electron microscopy (SEM) was used for visual characterization of the tested media.

2.2. Screening of commercial metal oxide nanoparticle material for arsenate adsorption

The arsenate adsorption capacity of the nanopowders was evaluated with "single-dose" screening batch adsorption experiments. Nanopowder suspensions containing 1 g/L nanopowder and ~1 mg/L As(V) as $Na_2HAsO_4{\cdot}7H_2O$ (reagent grade, Sigma–Aldrich) were prepared in 50 mL HDPE centrifuge vials that were pre-washed with 10% HNO_3 and triple rinsed with nanopure water. Table 2 summarizes the four waters used to prepare the suspensions. Three waters with chemistries occurring in the environment (surface water, ground water and treated water) were used in addition to 10 mM $NaHCO_3$ buffered nanopure water. Because the nanopure water and groundwater were not exposed to air before being used in experiments, their pH values (Table 2) varied slightly due to equilibration with atmospheric CO_2. The centrifuge vials were gently agitated for 3 days to allow proper mixing and establishment of adsorption pseudo-equilibrium [23–25]. The supernatant was pipetted and the concentration of unadsorbed arsenate was determined using an ET-AAS Varian Zeeman Spectra 400.

2.3. Isotherm experiments with the commercial metal oxide nanopowders

To select one nanopowder media, the adsorption capacities of the four commercial nanopowders exhibiting the highest arsenate removal in the screening experiments were further studied through isotherm experiments in 10 mM $NaHCO_3$ buffered nanopure water. No pH optimization experiments were conducted because the focus was removal of arsenate in natural waters, the majority of which have pH between of 6.5 and 8.5. Instead, experiments were conducted at pH values 8.4 ± 0.2 and 6.7 ± 0.3 to reflect typical boundary values. Isotherms were determined by adding 0.05–8 g/L of the metal oxide nanopowders to a solution that initially contained 1 mg/L arsenic. The pH was adjusted using KOH and HNO_3.

2.4. "Single-dose" batch adsorption experiments with commercial aggregated nanoparticle media

Since TiO_2 was the best performing metal oxide in the nanopowder experiments, commercially available nanoparticle aggregates containing TiO_2 were obtained for further study of arsenate adsorption. Table 3 summarizes the characteristics of these aggregates, which have different types of binders and were obtained from Dow Chemicals and Hydroglobe/Grover Technologies.

"Single-dose" batch adsorption experiments with nanoparticle aggregates were conducted using (1) a low dose with C (media) = 10 mg/L; and (2) a high dose with C (media) = 20 mg/L. The initial As(V) concentration was 100 μg/L, and the contact time was 7 days. Nanopure water buffered with 10 mM $NaHCO_3$ (pH 8.4 ± 0.2) was used as a model water matrix. To evaluate the effect of nanoparticle aggregate size on adsorption, four media sizes were used: (1) US mesh 20 × 30; (2) 30 × 60; (3) 60 × 80; and (4) 100 × 140.

Based on the findings from the nanoparticle characterization experiments, the nanoparticle aggregates were separated from the suspension by filtration through an 0.2 μm nylon membrane filter. The non-adsorbed arsenate concentration in the filtrate was determined using ET-AAS.

2.5. Isotherm experiments with commercial aggregated nanoparticle media

Although complete adsorption of arsenate onto TiO_2 can be achieved within the first few hours of contact, the contact time was extended to 10 days to ensure that complete pseudo-equilibrium was achieved inside the pores of the aggregated nanoparticle media. Isotherm experiments were conducted in 10 mM $NaHCO_3$ buffered nanopure water at pH was 8.4 ± 0.1.

Table 3
Characteristics of the evaluated aggregated nanoparticle media as provided by the manufacturers

Media (manufacturer)	Binder classification	Nature of the binder	Mesh size	Total pore area (m^2/g)	Titanium content (wt%)	Amount binder	pH_{IEP}
Adsorbsia GTO (DOW chemical)	Inorganic binder	Silica based	16 × 60	70	56.4	<19%	5.7
MetsorbG (hydroglobe)	Organic binder	Unknown	16 × 60	100–150	49.9	<16%	5.8

Nanoparticle aggregate doses ranged from 10 to 100 mg/L, and the initial arsenate concentration was ~100 μg/L. The nanoparticle aggregate sizes in the experiments were: (1) US mesh 20 × 30; (2) 30 × 60; and (3) 60 × 80. The separation and analysis procedures were the same as those for the "single-dose" batch experiments.

2.6. Short bed column experiments with commercial aggregated nanoparticle media

Fixed Bed Column (FBC) tests have been widely used to predict the performance of full-scale fixed bed absorbers and to evaluate the mass transport parameters of many single or multi-component contaminants [26–37]. Short Bed Adsorber columns (SBA), a special branch of the FBCs, have been demonstrated to be effective for estimating mass transport parameters [38]. An SBA column is a fixed bed column with a bed of sufficiently short length that immediate concentration breakthrough occurs [39]. SBAs simulate the adsorption-related activities occurring in the top layer of a full fixed bed adsorber. Although the dynamic behavior of an SBA usually does not allow visualization of the entire active adsorption zone as it moves through the bed, it can be useful for estimating mass transport parameters and for determining whether kinetics or media capacity is the limiting factor [32].

SBA tests were used to demonstrate that aggregated nanoparticle media would allow rapid mass transport of arsenate in a fixed bed adsorber. Glass columns of length 30.5 cm and diameter 1.1 cm (Ace Glass) were packed with commercial aggregated nanoparticle media (mesh size 100 × 140) supported on silica glass wool. The column diameter to particle ratio was > 70. According to Benenati and Brosilow [40] and Chu and Ng [41], ratios > 20 are sufficiently large that the wall effect on mass transfer can be neglected. Groundwater from central Arizona with arsenic concentration of ~28 μg/L was used in these tests (Table 2); Table 4 summarizes column operation conditions.

3. Results and discussion

3.1. Commercial nanopowder media

3.1.1. Characterization of commercial nanopowders

Separation of nanopowders and nanoparticle aggregates containing adsorbed arsenate was critical to validating experimental procedures. Nanopowder separation test results indicated that both filtration through an 0.2 μm filter and centrifugation separated nanopowders from the suspension with removal efficiencies >99%. Filtration of the nanopowder suspension through a 2.5 μm filter yielded >90% removal, which indicates that the nanopowders consist of larger aggregates than the individual nanoparticle sizes reported by the vendor (Table 1). SEM visual analysis of the nanopowders confirmed this. As Fig. 1 shows for TiO_2, smaller nanoparticles are aggregated together to form larger particles >1 μm in size. These observations were consistent with similar observations reported in the literature [42–46].

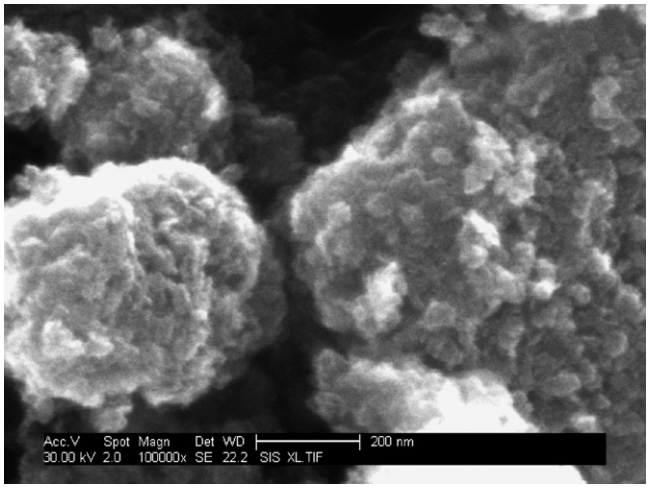

Fig. 1. Scanning electron microscope image of TiO_2 nanopowder.

3.1.2. Batch experiments

The screening "single-dose" batch experiments presented in Fig. 2 suggest that most nanopowders removed >90% of the arsenate for almost all water matrices. A slight reduction in arsenate removal efficiency often occurred in groundwater. As illustrated in Fig. 2, TiO_2, ZrO_2, Fe_2O_3 and NiO exhibited the highest arsenate removal in all water matrices, achieving >98% efficiency except for ZrO_2 in the groundwater matrix.

The screening tests initially indicated that MgO was one of the best performing nanopowders. The rapid increase in pH after its addition and the formation of easily settleable floc indicated that MgO nanopowder may be dissolving and reprecipitating as a hydroxide rather than removing arsenate by adsorption onto the MgO surface. MgO is relatively unreactive in bulk, but its

Table 4
Column operational conditions[a]

Column experiment	Final column height (cm)	Bed volume (mL)	Flow rate (mL/min)	$Re \times Sc$	EBCT (min)	Total bed volumes processed
C1	2.2	2.09	11	1000	0.28	43,267
C2	3.3	3.13	11	1000	0.28	42,468
C3	11.4	10.83	22	2000	0.50	26,228
C4	5.9	5.65	11	1000	0.50	25,971
C5	5.8	5.46	22	2000	0.25	30,233
C6	2.4	2.28	22	2000	0.10	27,204

[a] $Re = \nu\rho_l d_p/\mu_l$; $Sc = \mu_l/\rho_l D_l$, where ν is the hydraulic loading rate $[L][T]^{-1}$, ρ_l the density of water $[M][L]^{-3}$, d_p the adsorbent particle diameter [L], μ_l the viscosity of water $[M][L]^{-1}[T]^{-1}$ and D_l is the bulk liquid diffusivity for arsenate $[L]^2[T]^{-1}$ ($D_{As} = 10^{-5}$ cm^2/s).

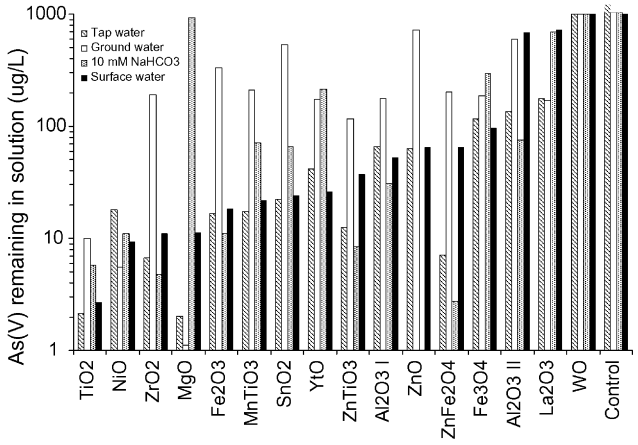

Fig. 2. Single-dose screening experiments for arsenic adsorption in surface water, ranked left-to-right $C_0(\mathrm{As}) \approx 1$ mg/L, C (nanopowder) = 1 g/L.

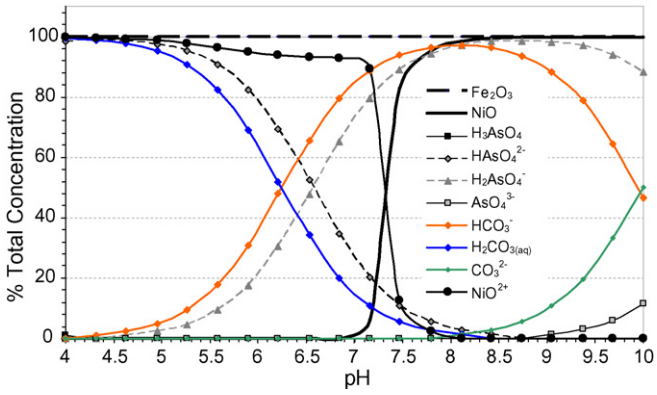

Fig. 3. Speciation of arsenate and bicarbonate and solubility of Fe_2O_3 and NiO in the presence of 10 mM $NaHCO_3$ and 1 mg/L As(V) as a function of pH.

reactivity markedly increases as particle size decreases [10]. Dissolution and reprecipitation as a hydroxide is also typical for the metal oxides of the IIIa group (La_2O_3 and Y_2O_3); these resemble Ca–Ba oxides and can absorb CO_2 and water to form carbonates and hydroxides [9]. In contrast to MgO, ZnO has amphotheric properties; depending on the pH, it can hydrolyze in water, releasing Zn^{2+} ions, or form zincanates [$Zn(OH)_3^-$] [10].

The reduced removal of arsenate in groundwater exhibited by Fe_2O_3 but not TiO_2 could be due to the presence of silica (~25 mg/L). Bang et al. [24] reported that silica concentrations of ~20 mg/L at neutral pH do not seriously impact arsenic adsorption by granular TiO_2. Several studies confirm, however, that silica can interfere with the adsorption of arsenic onto iron oxides by forming ferro-silicates [47–51]. Thus, the findings reported in Fig. 2 for Fe_2O_3 and TiO_2 nanopowder samples are consistent with those reported in the literature.

As Table 1 shows, the four nanopowders exhibiting the highest arsenate removal have isoelectric points between 5.9 and 10.7, which makes them slightly negatively to positively charged in the pH range of the tested water matrices. Considering the pK values for arsenate (pK_1 = 2.2; pK_2 = 6.8; and pK_3 = 11.6), this range of the isoelectric points should promote the adsorption of the dominant arsenate species ($HAsO_4^{2-}$ and $H_2AsO_4^-$, see Fig. 3) in natural waters with pH between 6.5 and 8.5 [50].

Fig. 3 also illustrates the solubility of Fe_2O_3 and NiO as a function of pH. TiO_2 and ZrO_2 are completely insoluble even in strong oxidizing acids. As such, MINEQL+ was used to model the solubility of Fe_2O_3 and NiO as a function of pH in presence of 10 mM $NaHCO_3$ and 1 mg/L Na_2HAsO_4. As shown in Fig. 3, the results suggest that Fe_2O_3 is stable and does not dissolve in pH 4–10. In contrast, NiO is stable at pH > 8.5 but tends to dissolve in waters with lower pH, releasing Ni^{2+}. This behavior makes NiO unsuitable as an adsorbent in natural waters.

Isotherm experiments on TiO_2, Fe_2O_3, NiO and ZrO_2 nanopowders supported the rankings from the "single-dose" screening experiments. As shown in Fig. 4, TiO_2 and ZrO_2 exhibit the highest adsorption capacity. The values for the fitted Freundlich isotherm ($q = KC_e^{1/n}$) parameter $1/n$ are all <0.55, indicating favorable adsorption processes for all four nanopowders (see Table 5). Furthermore, the isotherms indicate greater adsorption at lower pH, as illustrated in Fig. 4 suggesting better arsenate removal. Adsorption isotherm experiments for NiO at pH 6.7 ± 0.3 were not conducted due to its tendency to dissolve, however, and thus could not be compared to the others.

Based on data at different C_e values, ZrO_2 nanopowder appears to have better adsorption capacity than TiO_2 for solutions with lower As(V) concentrations (<10 μg/L), while the adsorption capacity of TiO_2 is better for solutions with higher As(V) concentrations (~1 mg/L). This behavior of ZrO_2 could be due to a different size distribution of the pores formed during nanopowder fabrication. Also, considering the affinity of ZrO_2 for carbon dioxide and carbonates, exposure of ZrO_2 to air and water containing these compounds may have reduced the active sites available for arsenate adsorption. Infrared spectroscopy studies have confirmed the formation of monodentate and bidentate inner-sphere complexes between ZrO_2 and HCO_3^- and/or CO_2 [52,53]. According to Dobson and McQuillan, [54] infrared spectra indicated formation of saturated monolayer coverage of HCO_3^- on the surface of ZrO_2 for solutions

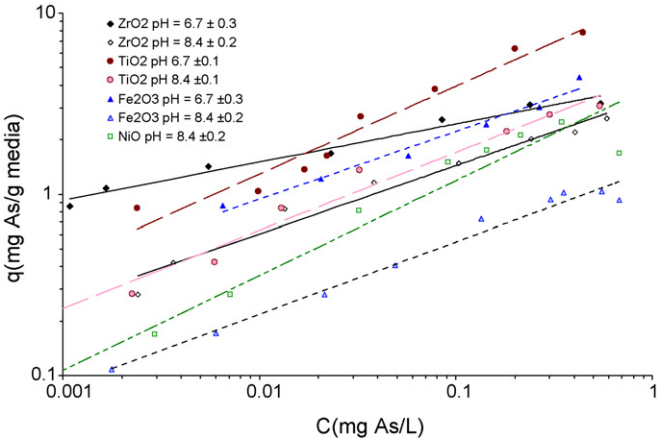

Fig. 4. Adsorption isotherms for the commercial nanopowders with the highest adsorption capacity. Water chemistry: $C_0(\mathrm{As}) \approx 1$ mg/L; 10 mM $NaHCO_3$ buffered water.

Table 5
Fitted Freundlich isotherm parameters[a] for the four nanopowders exhibiting highest arsenate removal

Nanopowder	K[b]		$1/n$		R^2	
	pH 6.7 ± 0.3	pH 8.4 ± 0.2	pH 6.7 ± 0.3	pH 8.4 ± 0.2	pH 6.7 ± 0.3	pH 8.4 ± 0.2
TiO_2	12.09	4.58	0.49	0.43	0.95	0.99
ZrO_2	3.97	3.42	0.21	0.38	0.97	0.97
Fe_2O_3	5.64	1.37	0.39	0.40	0.98	0.98
NiO	NA	3.96	NA	0.52	NA	0.95

[a] Freundlich equation: $q = KC_e^{1/n}$.
[b] Units $\left[\frac{\text{mg As/g(media)}}{(\text{mg As/L})^{1/n}}\right]$.

with $C(HCO_3^-) > 1$ mM and pH < 6.5; the layer could easily be removed by washing the ZrO_2 with NaOH solution at pH 12. Based on the pK values for bicarbonate (p$K_1 = 6.3$ and p$K_2 = 10.3$), HCO_3^- is the dominant species in waters with pH between 6.5 and 8.5, as illustrated in Fig. 3. The decrease in HCO_3^- adsorption in weak alkaline environments could explain the lower adsorption capacity of ZrO_2 than TiO_2 at higher As(V) concentrations as well as the slope of the ZrO_2 isotherm at pH ≈ 6.7 vs. pH ≈ 8.4. The potential adverse influence of carbonates on the ZrO_2 adsorption of arsenate was significant in the selection of TiO_2 for further study.

3.2. Commercial aggregated nanoparticle media

Because titanium-based nanopowders performed well in batch experiments, two commercially available TiO_2 aggregate nanoparticle media using different binders were tested (Table 3). Adsorbsia GTO and MetsorbG both have surface areas of 50–150 m^2/g and pH_{IEP} of 5.7–5.8, similar to the value of 5.9 for TiO_2 nanopowder (Table 1).

3.2.1. Batch experiments

Fig. 5 presents the results of batch experiments with two Adsorbsia GTO and MetsorbG dosages and four different media mesh sizes. The smallest diameter media (100 × 140) always adsorbed more arsenic than the largest (20 × 30) independent of dosage. For both media, even gentle agitation/mixing visibly led to some attrition and creation of smaller sized media. The lower arsenate removal by Adsorbsia GTO media could be related to its lower attrition compared to MetsorbG.

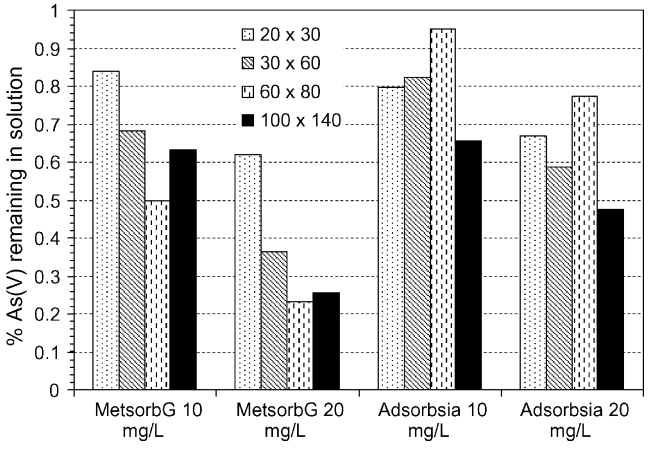

Fig. 5. Screening batch experiments for aggregated nanoparticle media at different loading concentrations and different mash sizes (C_0(As) ≈ 100 μg/L; 10 mM $NaHCO_3$; pH 8.2; contact time = 7 days).

Table 6 presents fitted Freundlich parameters (K and $1/n$) from isotherm experiments. The higher K values for MetsorbG indicate better arsenate removal, possibly due to its greater surface area. The K values of Adsorbsia GTO were lower than MetsorbG but similar to TiO_2 nanopowder (Table 5). Although the $1/n$ values for all media suggest favorable adsorption trends, the lower $1/n$ values for MetsorbG indicate more favorable adsorption. These adsorption capacity parameters suggest that the TiO_2 aggregates remove arsenate as well or better than TiO_2 nanopowder.

3.2.2. Short bed column experiments

In Fig. 6, effluent arsenate breakthrough is plotted against Bed Volumes (BV) of treated water for column tests on Adsorbsia GTO and MetsorbG at an EBCT of 0.28 min. Because the binders result in different bulk densities for the media, this plot indicates more BV were treated by Adsorbsia GTO than MetsorbG to reach the same effluent arsenate concentration. On a dry mass basis, however, the breakthrough curves are nearly identical (Fig. 7), suggesting a negligible role for the binder in arsenic adsorption. No significant media attrition was observed in any of these column tests.

Fig. 8 presents additional Adsorbsia GTO column test results. Three column tests were conducted at the same loading rate (flow rate = 22 mL/min) but different column lengths, which resulted in EBCTs of 0.1, 0.25 and 0.5 min (illustrated by solid symbols in the figure). As EBCT decreased, arsenic breakthrough occurred more quickly. In particular, at EBCTs of 0.1, 0.25 and 0.5 min, arsenic breakthrough began (i.e., $C_{As} > 1$ μg/L) at 3000, 6000, and 10,000 BVs, respectively. Even at an EBCT of 0.10 min, the short packed bed captured the entire mass transfer zone, suggesting rapid mass transfer kinetics and/or high external adsorption capacity. As a result, this media may be well suited for point of use systems, which operate at very short EBCTs.

A fourth column (EBCT = 0.5 min) was operated at a reduced flow rate (11 mL/min) and shorter bed depth to vary a mass transport calculated parameter, the Reynolds × Schmidt product value. Arsenic breakthrough was the same at the two loading rates tested (i.e. $Re \times Sc$ of 1000 and 2000), implying

Table 6
Fitted Freundlich isotherm parameters[a] for Adsorbsia GTO, and MetsorbG, in 10 mM $NaHCO_3$ buffered nanopure water, pH ≈ 8.4

Media	K[b]			$1/n$			R^2		
	20 × 30[c]	30 × 60[c]	60 × 80[c]	20 × 30[c]	30 × 60[c]	60 × 80[c]	20 × 30[c]	30 × 60[c]	60 × 80[c]
Adsorbsia GTO	28.45	8.83	7.08	0.97	0.59	0.49	0.95	0.85	0.98
MetsorbG	14.77	4.76	12.42	0.45	0.37	0.39	0.97	0.91	0.94

[a] Freundlich equation: $q = KC_e^{1/n}$.
[b] Units $\left[\frac{\text{mg As}/g(\text{media})}{(\text{mg As}/L)^{1/n}}\right]$.
[c] Mesh size.

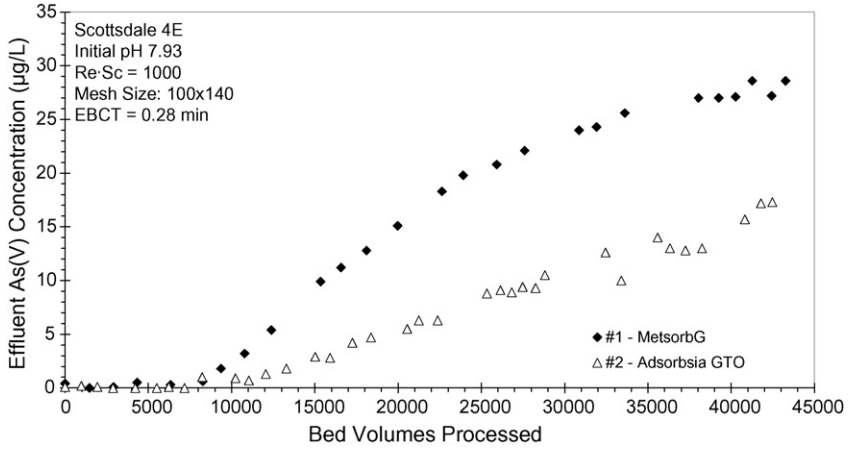

Fig. 6. Column tests on Adsorbsia GTO and MetsorbG (effluent concentration vs. bed volumes processed).

that intraparticle diffusion rather than external film diffusion controls arsenic mass transport.

3.3. Issues related to development of fixed bed columns packed with aggregated nanoparticle media

Attrition of nanoparticle aggregates or their binders could cause inadvertent releases of nanoparticles into treated water exiting continuous flow packed beds. The behavior of metal oxide nanoparticles in water environments and living organisms is not well understood. Evidence suggests that some nanoparticles can cause adverse effects in living organisms, however [55–58]. For example, a study by Sun et al. [59] shows that TiO_2 nanoparticles could facilitate arsenic accumulation in fish by adsorbing the toxin and transporting it inside the animal.

Therefore, some metal oxide nanoparticles with significant potential for arsenic removal may themselves pose a toxicity risk. Some metal oxide nanoparticles may end up in effluent simply by washing out of packed beds, but others may be dissolved in water prior to its treatment. For example, although NiO was thought to dissolve only in acidic environments, modeling in MINEQL+ and recent research indicate that

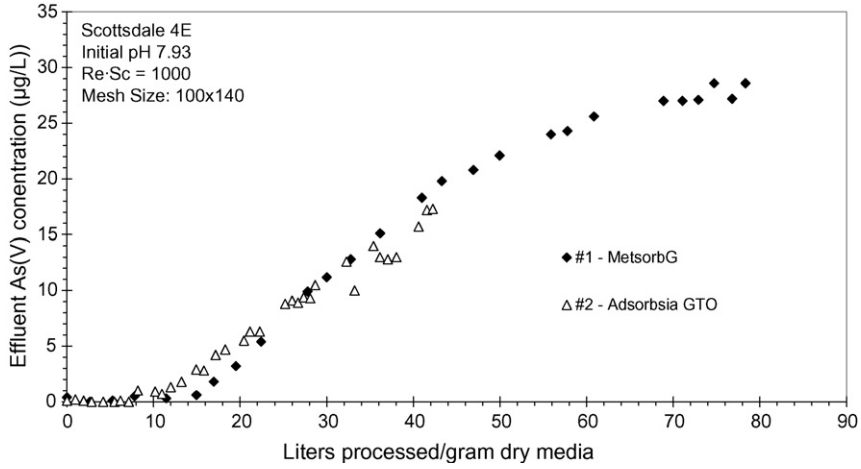

Fig. 7. Column tests on Adsorbsia GTO and MetsorbG (effluent concentration vs. liter processed/gram dry media).

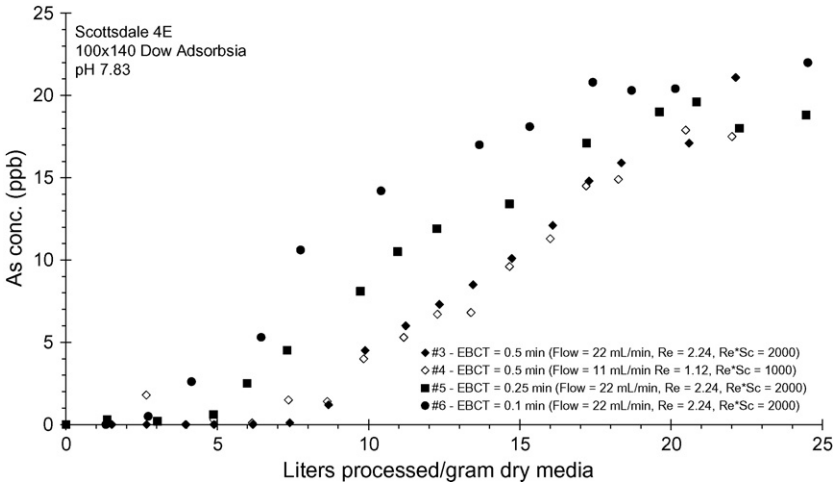

Fig. 8. Column tests on Adsorbsia GTO at variable hydraulic loadings.

it can dissolve in neutral pH water, resulting in Ni^{2+} release [60–62]. Ni^{2+} is a very toxic ion that causes serious health problems [63].

Binding agents for nanoparticle aggregation may also cause adverse effects due to poor agglomeration or simple toxicity. The amount of binder used in aggregation may also significantly decrease the surface area of the nanoparticles, resulting in media with lower rather than higher adsorption capacity.

The column experiments revealed several issues that may impact the performance of packed bed adsorbers using aggregated nanoparticle media. For instance, complete backwashing to remove fines from the packed bed was not possible due to potential loss of the media. This could translate into an inability to backwash all suspended solids found in the water during packed bed column treatment. In addition, aggregated nanoparticle media can reduce the porosity of and compress the packed bed, resulting in significant head loss and operational problems. Channeling, another efficiency-reducing problem that can result from compression of the packed bed, was noticeable during the short bed absorber test. Although the problems related to head loss, packed bed compression and channeling can be somewhat alleviated by increasing the diameter of the aggregated media, the results from the batch tests involving different media sizes suggest that this approach can reduce the adsorption capacity of the media.

4. Conclusion

Characterization of commercial nanopowders revealed that they consist of larger, aggregated particles (>1 μm). The screening single-dose batch experiments suggested that most nanopowders removed >90% of the arsenate for almost all water matrices under the given conditions. TiO_2, ZrO_2, Fe_2O_3 and NiO performed best, with removal efficiencies of >98% except for ZrO_2 in groundwater. The nanopowders have isoelectric points of 5.9–10.7, which makes them slightly negatively to positively charged in the pH range of the tested water matrices. The fitted Freundlich adsorption isotherm ($q = KC_e^{1/n}$) parameters for TiO_2, ZrO_2, Fe_2O_3 and NiO were K between 1.37 and 12.09 (mg As/g(media)) (L/mg As)$^{1/n}$ and $1/n$ between 0.21 and 0.52 at both pH ≈ 6.7 and 8.4 in 10 mM $NaHCO_3$ buffered nanopure water.

The single-dose batch experiments for different MetsorbG and Adsorbsia particle sizes indicated that attrition may impact arsenate removal. Their fitted Freundlich isotherm parameters (K of 4.75–28.45 (mg As/g(media)) (L/mg As)$^{1/n}$ and $1/n$ of 0.37–0.97) suggested favorable adsorption of arsenate in 10 mM $NaHCO_3$ buffered nanopure water. The higher K values for MetsorbG indicated better arsenate removal.

The SBA tests conducted on Adsorbsia GTO and MetsorbG at an EBCT = 0.28 min yielded nearly identical breakthrough curves when plotted on dry mass basis, suggesting a negligible role of the binder itself in adsorbing arsenic. At an EBCT of 0.10 min, the short packed bed captured the entire mass transfer zone, suggesting rapid mass transfer kinetics and/or high external adsorption capacity. As a result, this media may be well suited for point of use systems, which operate at very short EBCTs. SBA tests conducted at EBCT = 0.5 min and $Re \times Sc = 1000$ and 2000 implied that rapid intraparticle diffusion rather than external film diffusion controls arsenic mass transport.

Acknowledgments

The study was conducted with support from AWWARF Project #3077, DOW Chemicals, Hydroglobe/Grover Technologies, and the Environmental Technology Laboratory at Arizona State University Polytechnic Campus.

References

[1] R.F. Curl, R.E. Smalley, H.W. Kroto, S. O'Brien, J.R. Heath, How the news that we were not the first to conceive of soccer ball C-60 got to us, J. Mol. Graphics Model. 19 (2) (2001) 185–186.
[2] C.R. Martin, D.T. Mitchell, Nanomaterials in analytical chemistry, Anal. Chem. 70 (9) (1998) 322A–327A.
[3] The Bureau of National Affairs Inc., At NIOSH, Occup. Safety Health Rep. 35 (2) (2005) S-21.

[4] M.C. Roco, The emergence and policy implications of converging new technologies integrated from the nanoscale, J. Nanoparticle Res. 7 (2) (2005) 129–143.
[5] C.R. Yonzon, D.A. Stuart, X.Y. Zhang, A.D. McFarland, C.L. Haynes, R.P. Van Duyne, Towards advanced chemical and biological nanosensors—an overview, Talanta 67 (3) (2005) 438–448.
[6] J. Simon, Micro and nanotechnologies: dullish electrons and smart molecules, C. R. Chim. 8 (2005) 893–902.
[7] J.C. Glenn, Nanotechnology: Future military environmental health considerations, Technol. Forecast. Social Change 73 (2) (2006) 128–137.
[8] G.K. Stylios, P.V. Giannoudis, T. Wan, Applications of nanotechnologies in medical practice, Injury-Int. J. Care Injured 36 (2005) S6–S13.
[9] F.A. Cotton, G. Wilkinson, Advanced Inorganic Chemistry, Interscience Publishers, New York, NY, USA, 1972.
[10] N. Greenwood, A. Earnshaw, Chemistry of the Elements, 2nd ed., Reed Educational and Professional Publishing Ltd., Woburn, MA, USA, 1997.
[11] P.L. Smedley, D.G. Kinniburgh, A review of the source, behaviour and distribution of arsenic in natural waters, Appl. Geochem. 17 (5) (2002) 517–568.
[12] J. Matschullat, Arsenic in the geosphere—a review, Sci. Total Environ. 249 (2000) 297–312.
[13] P.K. Dutta, A.K. Ray, V.K. Sharma, F.J. Millero, Adsorption of arsenate and arsenite on titanium dioxide suspensions, J. Colloid Interf. Sci. 278 (2) (2004) 270–275.
[14] N.P. Nikolaidis, G.M. Dobbs, J. Chen, J.A. Lackovic, Arsenic mobility in contaminated lake sediments, Environ. Pollut. 129 (3) (2004) 479–487.
[15] US Department of Health and Human Services (Ed.), Toxicological profile for arsenic, US Department of Health and Human Services, Washington DC, 2000.
[16] Y.H. Xu, T. Nakajima, A. Ohki, Adsorption and removal of arsenic (V) from drinking water by aluminum-loaded shirasu-zeolite, J. Hazard. Mater. 92 (3) (2002) 275–287.
[17] R.D. Foust, P. Mohapatra, A.M. Compton-O'Brien, J. Reifel, Groundwater arsenic in the Verde valley in central Arizona, USA, Appl. Geochem. 19 (2) (2004) 251–255.
[18] R.J. Edmonds, D.J. Gellenbeck, Ground water quality in the west Salt River Valley, Arizona 1996–1998-relations to hydrogeology, water use, and land use No. 01-4126), USGS, Tucson, Arizona [Really no caps on the place names in the title?], 2002.
[19] US EPA, Arsenic in drinking water. Retrieved May 25, 2006 from http://www.epa.gov/safewater/arsenic.html.
[20] EU Council, Council directive 98/83/EC of 3 November 1998 on the quality of water intended for human consumption, Off. J. Eur. Commun. L 330 (1998) 32–54.
[21] WHO (Ed.), Guidelines for drinking-water quality, 3rd ed., World Health Organization, Geneva, 2004.
[22] US EPA, SW-846 test methods for evaluating solid waste, Physical/Chemical methods, US EPA, Washington DC, USA, 1996.
[23] M.E. Pena, G.P. Korfiatis, M. Patel, L. Lippincott, X. Meng, Adsorption of As (V) and As (III) by nanocrystalline titanium dioxide, Water Res. 39 (2005) 2327–2337.
[24] S. Bang, M. Patel, L. Lippincott, X.G. Meng, Removal of arsenic from groundwater by granular titanium dioxide adsorbent, Chemosphere 60 (3) (2005) 389–397.
[25] B. Manna, M. Dasgupta, U.C. Ghosh, Crystalline hydrous titanium (IV) oxide (CHTO): an arsenic (III) scavenger from natural water, J. Water Supply: Res. Technol.-AQUA 53 (7) (2004) 483–495.
[26] M.C. Carter, W.J. Weber, Modeling adsorption of TCE by activated carbon preloaded by background organic matter, Environ. Sci. Technol. 28 (1994) 614–623.
[27] D.W. Hand, J.C. Crittenden, D.R. Hokanson, J.L. Bulloch, Predicting the performance of fixed-bed granular activated carbon adsorbers, Water Sci. Technol. 35 (7) (1997) 235–241.
[28] D.R.U. Knappe, V.L. Snoeyink, P. Roche, M.J. Prados, M.M. Bourbigot, The effect of preloading on rapid small-scale column test predictions of atrazine removal by GAC adsorbers, Water Res. 31 (11) (1997) 2899–2909.
[29] D.D. Endicott, W.J. Weber, Lumped-parameter modeling of multicomponent adsorption in the treatment of coal-conversion wastewater by GAC, Environ. Prog. 4 (2) (1985) 105–111.
[30] P.B. Merkle, W.R. Knocke, D.L. Gallagher, J.C. Little, Dynamic model for soluble Mn^{2+} removal by oxide-coated filter media, J. Environ. Eng. -ASCE 123 (7) (1997) 650–658.
[31] W.J. Weber, Evolution of a technology, J. Environ. Eng. -ASCE 110 (5) (1984) 899–917.
[32] W.J. Weber, E.H. Smith, Simulation and design models for adsorption processes, Environ. Sci. Technol. 21 (11) (1987) 1040–1050.
[33] J.C. Crittenden, J.K. Berrigan, D.W. Hand, Design of rapid small-scale adsorption tests for a constant diffusivity, J. Water Pollut. Control Federat. 58 (4) (1986) 312–319.
[34] J.C. Crittenden, T.F. Speth, D.W. Hand, P.J. Luft, B. Lykins, Evaluating multicomponent competitive adsorption in fixed-beds, J. Environ. Eng. -ASCE 113 (6) (1987) 1363–1375.
[35] J.C. Crittenden, P.S. Reddy, H. Arora, J. Trynoski, D.W. Hand, D.L. Perram, et al., Predicting GAC performance with rapid small-scale column tests, J. Am. Water Works Assoc. 83 (1) (1991) 77–87.
[36] P. Westerhoff, D. Highfield, M. Badruzzaman, Y. Yoon, Rapid small-scale column tests for arsenate removal in iron oxide packed bed columns, J. Environ. Eng. -ASCE 131 (2) (2005) 262–271.
[37] A. Sperlich, A. Werner, A. Genz, G. Amy, E. Worch, M. Jekel, Breakthrough behavior of granular ferric hydroxide (GFH) fixed-bed adsorption filters: modeling and experimental approaches, Water Res. 39 (6) (2005) 1190–1198.
[38] E.H. Smith, W.J. Weber, Evaluation of mass-transfer parameters for adsorption of organic-compounds from complex organic matrices, Environ. Sci. Technol. 23 (6) (1989) 713–722.
[39] E.H. Smith, W.J. Weber, Modeling activated carbon adsorption of target organic-compounds from leachate-contaminated groundwaters, Environ. Sci. Technol. 22 (3) (1988) 313–321.
[40] R.F. Benenati, C.B. Brosilow, Void fraction distribution in bed of spheres, AIChE J. 8 (3) (1962) 351–361.
[41] C.F. Chu, K.M. Ng, Flow in packed tubes with a small tube to particle diameter ratio, AIChE J. 35 (1) (1989) 148–158.
[42] S. Gu, J. Onishi, Y. Kobayashi, D. Nagao, M. Konno, Preparation and colloidal stability of monodisperse magnetic polymer particles, J. Colloid Interf. Sci. 289 (2005) 419–426.
[43] H.F. Lecoanet, M.R. Wiesner, Velocity effects on fullerene and oxide nanoparticle deposition in porous media, Environ. Sci. Technol. 38 (16) (2004) 4377–4382.
[44] S. Dukhin, C. Zhu, R.N. Dave, Q. Yu, Hydrodynamic fragmentation of nanoparticle aggregates at orthokinetic coagulation, Adv. Colloid Interf. Sci. 114 (2005) 119–131.
[45] S.A. Chen, W.M. Liu, Preparation and characterization of surface-coated ZnS nanoparticles, Langmuir 15 (23) (1999) 8100–8104.
[46] Z. Zhang, P. Fenter, L. Cheng, N.C. Sturchio, M.J. Bedzyk, M.L. Machesky, et al., Zn^{2+} and Sr^{2+} adsorption at the TiO_2 (1 1 0)-electrolyte interface: influence of ionic strength, coverage, and anions, J. Colloid Interf. Sci. 295 (1) (2006) 50–64.
[47] C.C. Davis, H.W. Chen, M. Edwards, Modeling silica sorption to iron hydroxide, Environ. Sci. Technol. 36 (4) (2002) 582–587.
[48] C.C. Davis, W.R. Knocke, M. Edwards, Implications of aqueous silica sorption to iron hydroxide: mobilization of iron colloids and interference with sorption of arsenate and humic substances, Environ. Sci. Technol. 35 (15) (2001) 3158–3162.
[49] V. Lenoble, O. Bouras, V. Deluchat, B. Serpaud, J.C. Bollinger, Arsenic adsorption onto pillared clays and iron oxides, J. Colloid Interf. Sci. 255 (1) (2002) 52–58.
[50] X.G. Meng, S. Bang, G.P. Korfiatis, Effects of silicate, sulfate, and carbonate on arsenic removal by ferric chloride, Water Res. 34 (4) (2000) 1255–1261.
[51] G.S. Pokrovski, J. Schott, F. Garges, J.L. Hazemann, Iron (III)-silica interactions in aqueous solution: insights from X-ray absorption fine structure spectroscopy, Geochim. Cosmochim. Acta 67 (19) (2003) 3559–3573.

[52] W. Hertl, Surface-chemistry of zirconia polymorphs, Langmuir 5 (1) (1989) 96–100.
[53] B. Bachiller-Baeza, I. Rodriguez-Ramos, A. Guerrero-Ruiz, Interaction of carbon dioxide with the surface of zirconia polymorphs, Langmuir 14 (13) (1998) 3556–3564.
[54] K.D. Dobson, A.J. McQuillan, An infrared spectroscopic study of carbonate adsorption to zirconium dioxide sol–gel films from aqueous solutions, Langmuir 13 (13) (1997) 3392–3396.
[55] C.M. Sayes, J.D. Fortner, W. Guo, D. Lyon, A.M. Boyd, K.D. Ausman, et al., The differential cytotoxicity of water-soluble fullerenes, NanoLetters 4 (10) (2004) 1881–1887.
[56] G. Oberdorster, A. Maynard, K. Donaldson, V. Castranova, J. Fitzpatrick, K. Ausman, et al., Principles for characterizing the potential human health effects from exposure to nanomaterials: elements of a screening strategy, Particle Fibre Toxicol. 2 (2005) 8.
[57] G. Oberdorster, E. Oberdorster, J. Oberdorster, Nanotoxicology: an emerging discipline evolving from studies of ultrafine particles, Environ. Health Perspect. 113 (7) (2005) 823–839.
[58] G. Jia, H.F. Wang, L. Yan, X. Wang, R.J. Pei, T. Yan, et al., Cytotoxicity of carbon nanomaterials: single-wall nanotube, multi-wall nanotube, and fullerene, Environ. Sci. Technol. 39 (5) (2005) 1378–1383.
[59] H. Sun, X. Zhang, Y. Chen, Q. Qiu, J.C. Crittenden, Enhanced accumulation of arsenic in carp in the presence of titanium dioxide nanoparticles, Water Air Soil Pollut. 178 (2007) 245–254.
[60] C. Ludwig, W.H. Casey, On the mechanisms of dissolution of bunsenite [NiO (s)] and other simple oxide minerals, J. Colloid Interf. Sci. 178 (1) (1996) 176–185.
[61] C. Ludwig, J.L. Devidal, W.H. Casey, The effect of different functional groups on the ligand-promoted dissolution of NiO and other oxide minerals, Geochim. Cosmochim. Acta 60 (2) (1996) 213–224.
[62] P.R. Tremaine, J.C. Leblanc, The solubility of nickel-oxide and hydrolysis of Ni-2 (+) in water to 573-K, J. Chem. Thermodyn. 12 (6) (1980) 521–538.
[63] US Department of Health and Human Services, Toxicological profile for nickel, US Department of Health and Human Services, Washington DC, USA, 2005.